*Geol. Mag.* **140** (*6*), *2003, pp. 707–719.* © *2003 Cambridge University Press*
DOI: 10.1017/S0016756803008136 *Printed in the United Kingdom*


# Geothermal regime in the Qaidam basin, northeast Qinghai–Tibet Plateau

QIU NANSHENG*†

*Key Laboratory for Hydrocarbon Accumulation Mechanism, Ministry of Education, University of Petroleum, Beijing 102249, P. R. China
†Basin & Reservoir Research Centre, University of Petroleum, Fuxue Road, Changping County, Beijing 102249, P. R. China

(*Received* 23 October 2002; *accepted* 10 June 2003)

**Abstract** – The thermal properties of rocks in the upper crust of the Qaidam basin are given based on measurements of 98 thermal conductivities and 50 heat production values. Nineteen new measured heat flow data were obtained from thermal conductivity data and systematic steady-state temperature data. This paper contributes 28 calculated heat flow values for the basin for the first time. Examination of 47 heat flow values, ranging from 31.3 to 70.4 mW/m$^2$ with an average value of 52.6 $\pm$ 9.6 mW/m$^2$, gives the heat flow distribution character of the basin: high heat flows over 60 mW/m$^2$ are distributed in the western and central parts of the basin. Lower heat flow values are found in the eastern part and north marginal area of the basin, with values less 40 mW/m$^2$. The Qaidam basin heatflow data show a linear relationship between heatflow and heat production, based on thermal structure analysis. The thermal structure of the lithosphere is characterized as having a 'hot crust' but 'cold mantle'. Heat production in the upper crust is a significant source of heat in the basin and contributes up to 56.8 % of the surface heat flow. The heat flow province is of great geophysical significance, and the thermal structure of the area gives clues about the regional geodynamics. Study of the Qaidam basin thermal structure shows that the crust has been highly active, particularly during its most recent geological evolution. This corresponds to Himalayan tectonic movements during latest Eocene to Quaternary times in the region of the Qinghai–Tibet Plateau. Since the Qaidam basin is in the northeastern area of the Qinghai–Tibet Plateau, the heat flow values and the thermal structure of the basin may give some insight into the thermal state of the plateau, and study of thermal regime of the Qaidam basin could in turn provide useful information about the tectonics of the Qinghai–Tibet Plateau.

Keywords: heat flow, Qaidam basin, Qinghai–Tibet Plateau, thermal regime, thermal conductivity, heat production.

## 1. Introduction

The Qaidam basin, an orographic basin that formed primarily during Mesozoic and Cenozoic times, is a petroleum province on the northeastern Qinghai–Tibet Plateau, China. The basin, with an area of 129 000 km$^2$, is bounded by the Aljin Mountains to the northwest, the Qilian Mountains to the northeast, Qimantager Mountains to the southeast and East Kunlun Mountains to the southwest (Fig. 1). The elevations of the basin and the surrounding mountains range from 2700 m to 5000 m above sea-level. The basin developed on the pre-Mesozoic basement. It was tectonically active throughout the Cenozoic and underwent a complex structural evolution. The western and northern sub-basins reflect separate tectonic histories (Huang, Huang & Ma, 1996), which have resulted in different geological settings for the two parts of the basin. The Mesozoic and Cenozoic evolution of the western basin can be divided into four structural phases (Huang, 1993): (1) rift-subsidence during Mesozoic times, with the northern margin being uplifted at the end of the Cretaceous; (2) the Himalayan movement stage I at the end of Eocene times, resulting in rapid subsidence of the western basin; (3) the depression stage during Late Oligocene to Middle Pliocene times, when the entire basin subsided; and (4) the Himalayan movement stage II and stage III from Pliocene to Quaternary times, resulting in an unconformity at the base of the Quaternary.

The depositional centre of the basin shifted progressively towards the east during Cenozoic times. The shift was accompanied by uplift in the western part of the basin and subsidence in the east (Figs 1, 2). Cenozoic sediments are more than 10 000 m thick in the basin, but Quaternary strata occur mainly in the eastern part of the basin with a thickness of over 3000 m. Only a few boreholes have intersected the Mesozoic strata at the western basin margin. The Upper Pliocene and Quaternary strata were eroded away in most parts of the western basin. However, most Tertiary sediments

* Address for correspondence: Basin & Reservoir Research Centre, University of Petroleum, Changping County, Beijing 102249, P. R. China; e-mail: qiunsh@bjpeu.edu.cn

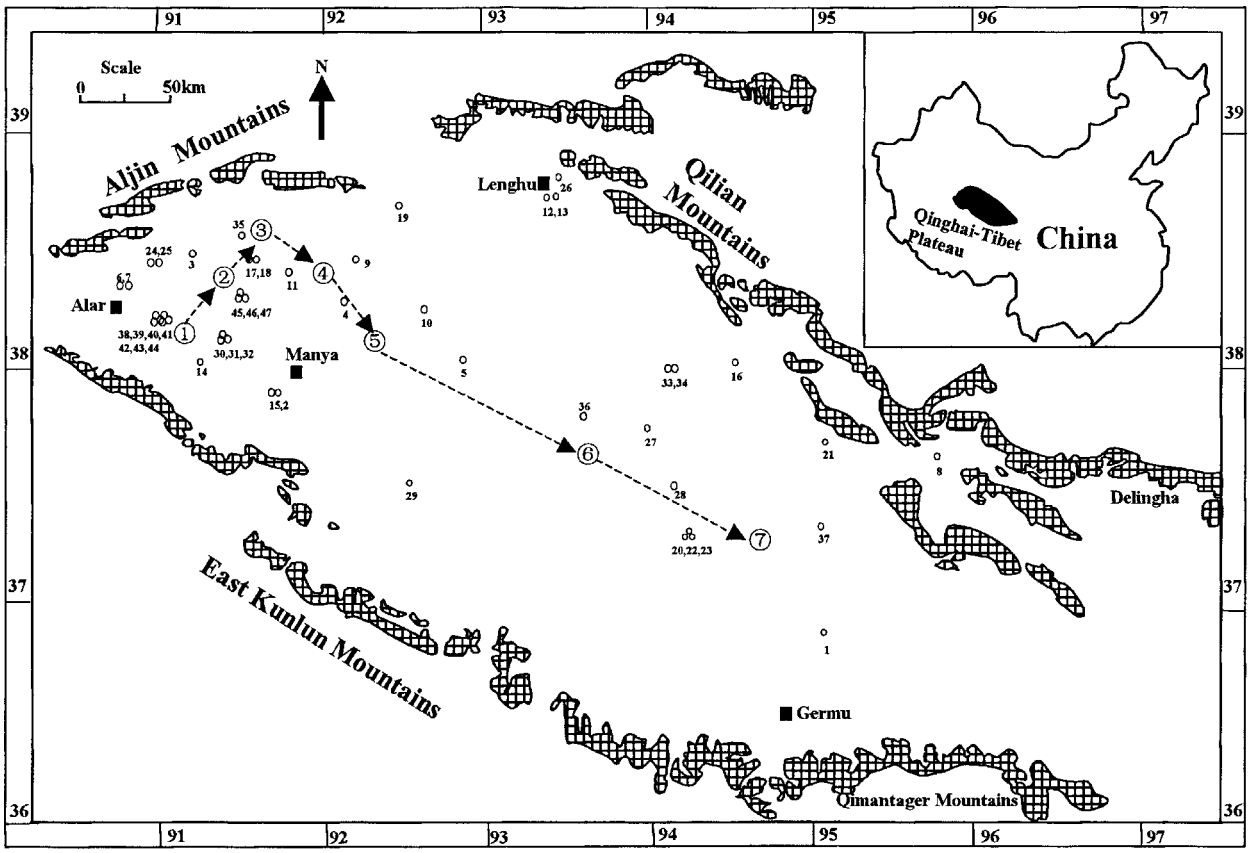


Figure 1. Locations of the wells used in this study in the Qaidam basin. The circled numbers are deposition centres at different geological time (see Fig. 2). The map grid gives degrees of latitude and longitude.

| Series | Group | Lithology | Thickness(m) | Deposition Centre | K(W/m.K) | A ($\mu$ W/m$^3$) |
|---|---|---|---|---|---|---|
| Quaternary | Qigequan | | 0-200m | ⑦ | 0.85±0.25 | 2.21±0.58 |
| Pliocene | Shizigou | | 0-1500m | ⑥ | 1.89 ±0.68 | 2.28±0.42 |
| | U.Youshashan | | 0-1500m | ⑤ | | |
| | L.Youshashan | | 600-2000m | ④ | | |
| Miocene | U.Ganchaigou | | 500-1200m | ③ | 1.90 ±0.40 | 2.34±0.33 |
| Oligocene | L.Ganchaigou | | 850-1575m | ② | 2.37 ±0.70 | 2.01±0.50 |
| Palaeocene-Eocene | Lulehe | | 300-1237m | ① | | |
| Cretaceous-Jurassic | | | 7500m | | 2.11 ±0.71 | 1.69±0.67 |

Conglomerate Sandstone Mudstone Shale Sandy conglomerate Sandy mudstone

Figure 2. Stratigraphic column for the Qaidam basin. K is the value of thermal conductivity, and these data are bulk conductivity values, shown as mean values ± one standard deviation. A is radiogenic heat production rate. The deposition centres are shown in Figure 1.

were eroded away along the northern basin margin. As a result, the Mesozoic strata occur only in the northern basin and were buried to relatively shallow depths.

The Mesozoic and Cenozoic sedimentary succession is composed of sandstone, shale and calcareous rocks. There are three hydrocarbon source intervals: the Jurassic Xiaomeigou and Dameigou groups in the northern basin, the Oligocene Lower Ganchaigou and Miocene Upper Ganchaigou groups in the western basin and the Quaternary Qigequan Group in the eastern basin. These source rocks are dominated by shale and mudstone, deposited in lake and salty-lake environments. Shale and calcareous rocks are mostly developed in the basin, and have acted as seal formations. They also influence the temperature distribution within the basin. All the reservoir rocks are sandstones within the Oligocene Lower Ganchaigou, the Miocene–Pliocene Lower and Upper Youshashan and Shizigou groups in the western basin, the Qigequan Group in the eastern basin and the Dameigou and Xiaomeigou groups in the northern basin.

Although the stratigraphy and structure of the Qaidam basin have been well studied (Huang, 1993; Huang, Huang & Ma, 1996), little has been published about the geothermal regime during the evolution of the basin. Some thermal studies of the basin have focused on using the bottom-hole temperature (BHT) data to analyse the thermal conditions in the basin (Wang *et al*. 1990). Other thermal studies used the steady-state temperature data to evaluate the thermal state of the basin, and 22 heat flow values and a geothermal gradient map were obtained (Shen *et al*. 1994*a*). Ideally, to obtain a high quality temperature log, a well should not be disturbed. The temperature

https://doi.org/10.1017/S0016756803008136 Published online by Cambridge University Press

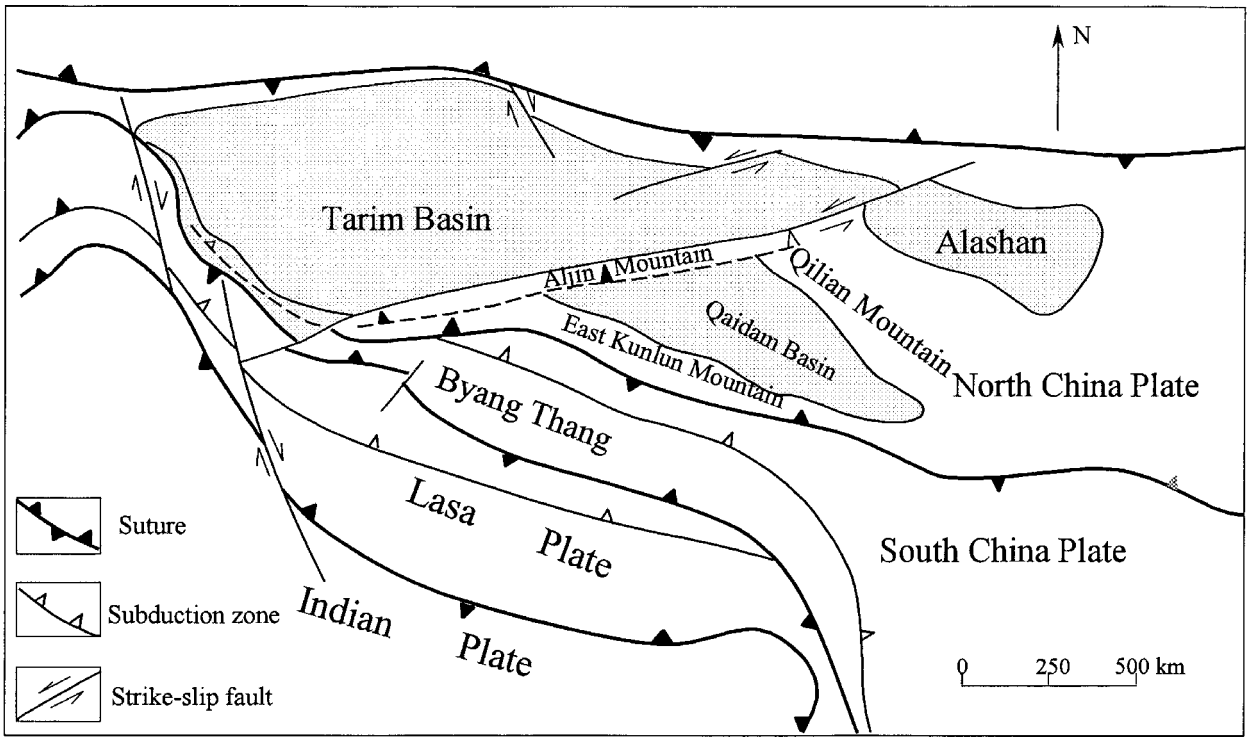


Figure 3. Location of the Qaidam basin in the Qinghai–Tibet Plateau.

of the borehole fluid and the surrounding rocks should recovered from thermal perturbations created by fluid movement in and around the well bore.

The thermal history of the basin has been derived primarily from the vitrinite reflectance and fluid inclusion data (Ren, 1993; Shen *et al*. 1994*b*). Shen & Wang (1995) calculated the timing of petroleum maturation using time–temperature index (TTI) methods and a vitrinite reflectance kinetic model. The results of burial history modelling indicated a rapid subsidence of the basin during Late Pliocene to Quaternary times, which caused the main hydrocarbon source rocks to move into and pass through the oil and gas maturity phases during this time interval. More recently, Qiu (2002) reconstructed the thermal evolution history based on apatite fission track and vitrinite reflectance data.

In order to study the thermal regime of the Qaidam Basin, the thermal properties of the rocks must be determined. G. H. Li obtained numerous measurements of thermal conductivity and heat production (G. H. Li, unpub. Masters thesis, Institute of Geology, Academia Sinica, 1992). In this study, 98 thermal conductivity measurements and 50 heat generation measurements of rocks were carried out, and these data are the basis for investigating current thermal patterns and the thermal structure of the basin.

The regional tectonic evolution of the Qaidam basin is related to the tectonic evolution of the entire Qinghai–Tibet Plateau. Since it is situated on the northeastern Qinghai–Tibet Plateau (Fig. 3), the formation and evolution of the Qaidam basin correlates with the Alpine tectonic cycle and the Tethys-Himalayan tectonic domain, which controls the Qinghai–Tibet Plateau uplift. When the Indian Plate and Palaeo-Asian Plate collided, the extrusion stress resulted in the formation of the Kunlun and Himalayan mountain belts and strong uplift of the Qinghai–Tibet Plateau. The Qaidam basin was formed by the extrusion stress (Gao & Zhao, 2001). Analysis of the tectonics and deep lithosphere structure of the Qaidam basin may provide useful information regarding both the evolution of the basin and the tectonic movement of the Qinghai–Tibet Plateau. The thermal regime and thermal history of the basin may say something not only about the regional tectonic characteristics and deep lithosphere structure of the basin, but also about the deep thermal structure and tectonic evolution of the Qinghai–Tibet Plateau.

This paper discusses the heat flow distribution and thermal structure of the Qaidam basin based on temperature data and the detailed thermal properties of the rocks, providing a basis for study of the regional tectonic characteristics of the basin and the Qinghai–Tibet Plateau.

## 2. Samples and experiments

### 2.a. Thermal conductivity

Thermal conductivity is an important parameter of heat flow measurements. There are two types of methods used to measure thermal conductivity: one-dimensional (linear) steady-state and two-dimensional (cylindrical)

https://doi.org/10.1017/S0016756803008136 Published online by Cambridge University Press

Table 1. Thermal conductivity (K) measurement data used in this study

| No. | Wells | Depth (m) | Age | Lithology | K (W/m · K) | No. | Wells | Depth (m) | Age | Lithology | K (W/m · K) |
|---|---|---|---|---|---|---|---|---|---|---|---|
| 1 | Han-2 | 1955 | Pliocene | Mudstone | 1.803 ± 0.15 | 52 | Shidi-22 | 472 | Jurassic | Siltstone | 1.131 ± 0.17 |
| 2 | | 2456 | Pliocene | Mudstone | 2.496 ± 0.24 | 53 | | 582 | Jurassic | Sandstone | 1.079 ± 0.31 |
| 3 | | 3352 | Pliocene | Mudstone | 1.849 ± 0.11 | 54 | | 672 | Jurassic | Siltstone | 1.740 ± 0.21 |
| 4 | | 4245 | Pliocene | Mudstone | 2.118 ± 0.19 | 55 | | 742 | Jurassic | Sandstone | 1.670 ± 0.20 |
| 5 | | 4608 | Pliocene | Siltstone | 4.226 ± 0.38 | 56 | | 1148 | Jurassic | Sandstone | 1.787 ± 0.06 |
| 6 | | 4875 | Pliocene | Siltstone | 2.195 ± 0.11 | 57 | Wanxi-1 | 975 | Miocene | Mudstone | 2.512 ± 0.28 |
| 7 | Hongshancan-1 | 910 | Cretaceous | Sandstone | 2.490 ± 0.32 | 58 | | 2778 | Oligocene | Siltstone | 1.940 ± 0.08 |
| 8 | | 1588 | Jurassic | Sandstone | 2.658 ± 0.32 | 59 | | 2823 | Oligocene | Siltstone | 3.156 ± 0.55 |
| 9 | | 1642 | Jurassic | Sandstone | 1.316 ± 0.11 | 60 | | 3098 | Eocene | Siltstone | 2.063 ± 0.75 |
| 10 | | 2100 | Jurassic | Sandstone | 1.269 ± 0.22 | 61 | Yacan-3 | 2080 | Pliocene | Sandstone | 2.857 ± 0.40 |
| 11 | Jian-2 | 1784 | Pliocene | Marl | 1.688 ± 0.25 | 62 | | 2383 | Pliocene | Siltstone | 1.733 ± 0.12 |
| 12 | | 1844 | Pliocene | Mudstone | 1.975 ± 0.11 | 63 | | 2653 | Pliocene | Siltstone | 1.806 ± 0.11 |
| 13 | | 1934 | Pliocene | Mudstone | 1.407 ± 0.28 | 64 | | 3710 | Pliocene | Siltstone | 1.645 ± 0.11 |
| 14 | | 2152 | Pliocene | Mudstone | 1.912 ± 0.39 | 65 | | 4277 | Pliocene | Siltstone | 2.647 ± 0.50 |
| 15 | | 2265 | Pliocene | Mudstone | 2.356 ± 0.31 | 66 | You-6 | 2400 | Miocene | Sandstone | 1.683 ± 0.45 |
| 16 | | 2700 | Pliocene | Sandstone | 1.925 ± 0.90 | 67 | | 3002 | Oligocene | Sandstone | 2.902 ± 0.20 |
| 17 | | 2867 | Pliocene | Sandstone | 3.148 ± 0.41 | 68 | | 3378 | Oligocene | Sandstone | 4.375 ± 0.48 |
| 18 | | 3243 | Pliocene | Sandstone | 2.641 ± 0.13 | 69 | | 4311 | Oligocene | Sandstone | 3.437 ± 0.70 |
| 19 | | 3313 | Pliocene | Sandstone | 2.694 ± 0.53 | 70 | Yue-12 | 1200 | Oligocene | Mudstone | 1.381 ± 0.25 |
| 20 | | 3500 | Pliocene | Sandstone | 2.955 ± 0.19 | 71 | | 1687 | Oligocene | Sandstone | 1.055 ± 0.06 |
| 21 | | 4098 | Pliocene | Mudstone | 1.871 ± 0.10 | 72 | | 1788 | Oligocene | Sandstone | 1.865 ± 0.26 |
| 22 | | 4500 | Pliocene | Sandstone | 3.193 ± 0.51 | 73 | | 1815 | Oligocene | Sandstone | 3.319 ± 0.42 |
| 23 | Nan-4 | 103 | Pliocene | Mudstone | 0.810 ± 0.10 | 74 | Yue-58 | 1780 | Pliocene | Sandstone | 1.877 ± 0.49 |
| 24 | | 166 | Pliocene | Mudstone | 0.857 ± 0.09 | 75 | | 1945 | Pliocene | Sandstone | 2.502 ± 0.39 |
| 25 | | 238 | Pliocene | Mudstone | 0.882 ± 0.09 | 76 | | 2020 | Miocene | Sandstone | 1.601 ± 0.05 |
| 26 | | 803 | Pliocene | Mudstone | 0.961 ± 0.07 | 77 | | 2130 | Miocene | Sandstone | 2.367 ± 0.07 |
| 27 | | 912 | Pliocene | Mudstone | 1.696 ± 0.15 | 78 | Yue-119 | 3253 | Oligocene | Sandstone | 2.733 ± 0.15 |
| 28 | | 1070 | Pliocene | Mudstone | 1.269 ± 0.37 | 79 | | 3330 | Oligocene | Sandstone | 3.600 ± 0.25 |
| 29 | | 1220 | Pliocene | Mudstone | 1.497 ± 0.13 | 80 | | 3425 | Oligocene | Sandstone | 3.133 ± 0.10 |
| 30 | Nan-5 | 3020 | Miocene | Mudstone | 2.715 ± 0.19 | 81 | | Outcrop | Jurassic | Sandstone | 1.762 ± 0.22 |
| 31 | Saishen-1 | 1022 | Miocene | Sandstone | 1.369 ± 0.20 | 82 | | Outcrop | Cretaceous | Sandstone | 1.860 ± 0.20 |
| 32 | | 1100 | Miocene | Sandstone | 2.501 ± 0.37 | 83 | | Outcrop | Jurassic | Sandstone | 3.068 ± 0.45 |
| 33 | | 1175 | Miocene | Sandstone | 1.623 ± 0.05 | 84 | | Outcrop | Jurassic | Sandstone | 2.389 ± 0.27 |
| 34 | | 1273 | Miocene | Sandstone | 1.113 ± 0.17 | 85 | | Outcrop | Jurassic | Shale | 0.439 ± 0.12 |
| 35 | | 1360 | Miocene | Sandstone | 1.320 ± 0.14 | 86 | | Outcrop | Carbonif. | Limestone | 3.910 ± 0.28 |
| 36 | | 1460 | Miocene | Limestone | 1.605 ± 0.10 | 87 | | Outcrop | Devonian | Congl. | 5.708 ± 1.32 |
| 37 | | 1565 | Oligocene | Sandstone | 1.350 ± 0.21 | 88 | | Outcrop | Carbonif. | Limestone | 3.209 ± 0.62 |
| 38 | | 1650 | Oligocene | Mudstone | 3.246 ± 0.40 | 89 | | Outcrop | Sinian | Dolomite | 3.149 ± 0.52 |
| 39 | Sezhong-6 | 393 | Quaternary | Mudstone | 0.602 ± 0.10 | 90 | | Outcrop | Ordovician | Limestone | 2.847 ± 0.32 |
| 40 | | 463 | Quaternary | Mudstone | 0.766 ± 0.13 | 91 | | Outcrop | Ordovician | Sandstone | 4.140 ± 1.22 |
| 41 | | 518 | Quaternary | Mudstone | 0.712 ± 0.10 | 92 | | Outcrop | Carbonif. | Sandstone | 3.329 ± 0.60 |
| 42 | | 585 | Quaternary | Mudstone | 0.726 ± 0.17 | 93 | | Outcrop | Triassic | Tuff | 4.193 ± 1.26 |
| 43 | | 643 | Quaternary | Mudstone | 0.981 ± 0.28 | 94 | | Outcrop | Triassic | Sandstone | 2.732 ± 0.55 |
| 44 | | 740 | Quaternary | Mudstone | 0.727 ± 0.10 | 95 | | Outcrop | Proterozoic | Marble | 2.426 ± 0.35 |
| 45 | | 833 | Quaternary | Mudstone | 0.839 ± 0.08 | 96 | | Outcrop | Sinian | Sandstone | 4.634 ± 2.00 |
| 46 | | 955 | Quaternary | Siltstone | 1.575 ± 0.33 | 97 | | Outcrop | Ordovician | Sandstone | 3.473 ± 078 |
| 47 | | 1060 | Quaternary | Mudstone | 0.890 ± 0.01 | 98 | | Outcrop | Proterozoia | Phyllite | 1.612 ± 0.20 |
| 48 | Shi-23 | 3998 | Oligocene | Mudstone | 2.551 ± 0.55 | | | | | | |
| 49 | | 4025 | Oligocene | Sandstone | 2.476 ± 0.41 | | | | | | |
| 50 | | 4060 | Oligocene | Sandstone | 2.081 ± 0.20 | | | | | | |
| 51 | | 5510 | Eocene | Sandstone | 2.428 ± 0.17 | | | | | | |

transient methods. For this study, thermal conductivities were tested at room temperature using a steady-state divided bar type Geotherm-II model thermal conductivity meter, provided by the Institute of Geology, Academia Sinica. Each sample was tested three times under the same conditions. The thermal conductivity value of each sample was obtained by using the weighted average value of the three measured data.

Eighty core and 18 outcrop samples were measured to obtain 98 thermal conductivity (K) values for this study (Table 1). The core samples were taken from the Jurassic to Quaternary succession at burial depths of 102 to 5683 m, and they consist of shale, siltstone and sandstone. The outcrop samples were collected from Sinian- to Cretaceous-age exposures. The Palaeozoic samples are composed of sandstone, conglomerate, crystalline limestone and dolomites, however, the Precambrian samples are dominated by sandstone, marble and phyllite. Figure 4 shows the relationship between thermal conductivity values and depth of samples in the Qaidam basin with the data from Li (G. H. Li, unpub. Masters thesis, Institute of Geology, Academia Sinica, 1992) incorporated into the diagram. Here, the lithologic type 'mudstone' in fact includes mudstone, shale and sandy mudstone; the lithologic 'sandstone' includes sandstone, siltstone, conglomerate and muddy sandstone. The mudstone

https://doi.org/10.1017/S0016756803008136 Published online by Cambridge University Press

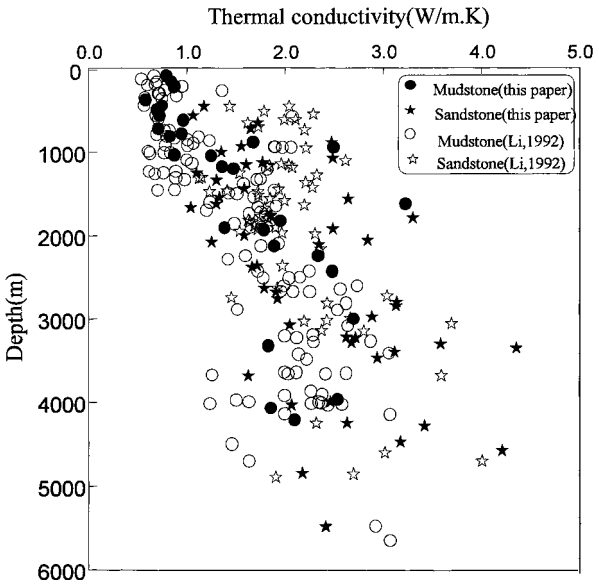


Figure 4. Thermal conductivity values of Cenozoic core samples in the basin. 'Li, 1992' refers to 'G. H. Li, unpub. Masters thesis, Institute of Geology, Academia Sinica, 1992'.

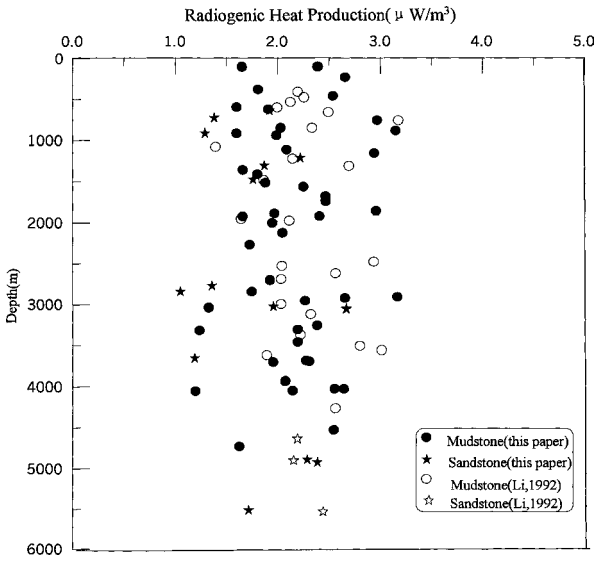


Figure 5. Heat production data for core samples in the basin.

produces lower thermal conductivity values than the sandstone, and thermal conductivity increases with the age of the Cenozoic samples (Fig. 6). The thermal conductivity of water-undersaturated samples and the measurement errors for each stratigraphic interval are listed in Figure 2.

We did not correct the results to ambient stratigraphic temperature conditions. The average error can be as high as 5–10 % for a 100 °C temperature increase in granite and carbonate rocks, according to Robertson (1988). A water saturation correction for thermal conductivity was made by using the data for samples saturated with water provided by Li (G. H. Li, unpub. Masters thesis, Institute of Geology, Academia Sinica, 1992).

### 2.b. Heat production

Heat produced by the decay of radioactive elements in rocks is the main internal heat source within the Earth. All natural radioactive isotopes generate heat to a certain extent, but only the decay series of uranium and thorium and the nuclide $^{40}$K are geologically significant heat-producing elements, since they have relatively high abundance, relatively high heat production rate and long half-lifes. This study used $\gamma$-ray spectrometry, spectrophotometry and isotope dilution for testing the concentrations of uranium and thorium and atomic absorption for potassium measurement. The heat production is calculated by applying the formula of Touloukian & Dewitt (1972) based on analysis of U, Th and K concentrations in rocks:

$$A = 10^{-5}\rho\,(9.52C_{\mathrm{U}} + 2.56C_{\mathrm{Th}} + 3.48C_{\mathrm{K}}) \qquad (1)$$

where $A$ is the radiogenic heat production ($\mu$W/m$^3$), $\rho$ is the density of rocks (g/cm$^3$), and $C_{\mathrm{U}}$ (ppm), $C_{\mathrm{Th}}$ (ppm) and $C_{\mathrm{K}}$ (%) are the concentrations of uranium, thorium and potassium elements in the rocks, respectively.

Forty-one core samples and nine outcrop samples were tested in this part of the study. The sample details are given in Table 2. Heat production values of core samples lie between 1.07 and 3.13 $\mu$W/m$^3$ with an average of 2.09 $\mu$W/m$^3$. As shown in Figure 5, heat production values are higher for mudstone than sandstone. However, the statistical mean of radiogenic heat production in each stratigraphic interval indicates that the heat production changes little in the Cenozoic. The Miocene rocks display the highest radiogenic heat production due to their greater proportion of mudstone (Fig. 6). Within the Cenozoic stratigraphic interval, however, the heat production distribution is taken to be uniform, as depicted in Figure 6. The Cenozoic strata have an average value of 2.2 $\mu$W/m$^3$. The Mesozoic samples have lower values with an average of 1.69 $\mu$W/m$^3$.

## 3. Heat flow distribution

Heat flow values are calculated from the thermal gradient and thermal conductivity of the corresponding depth intervals. Beck & Balling (1988) suggested that for a valid heat flow value, the equilibrium temperature gradient should be obtained in combination with values for the thermal properties of materials through which temperature gradients had been measured. However, in practice it is not easy to obtain reliable heat flow values for two reasons. First, the temperature measurement should be in near steady-state. During drilling, the temperature field was greatly disturbed. Many other effects could perturb measured temperatures significantly,

https://doi.org/10.1017/S0016756803008136 Published online by Cambridge University Press

Table 2. Radiogenic heat production (A) measurement data used in this study

| No. | Well | Depth (m) | Age | Lithology | U (ppm) | Th (ppm) | K (%) | $\rho$ (g/cm$^3$) | A ($\mu$W/m$^3$) |
|---|---|---|---|---|---|---|---|---|---|
| 1 | Dun-5 | 2505 | Pliocene | Mudstone | 5.78 | 9.74 | 1.97 | 2.50 | 2.17 |
| 2 | | 3098 | Pliocene | Mudstone | 5.91 | 11.22 | 3.94 | 2.50 | 2.47 |
| 3 | Feng-3 | 2667 | Pliocene | Mudstone | 5.76 | 7.22 | 3.84 | 2.50 | 2.17 |
| 4 | | 3539 | Pliocene | Mudstone | 7.06 | 10.82 | 4.71 | 2.50 | 2.78 |
| 5 | Han-2 | 1955 | Pliocene | Mudstone | 4.34 | 14.98 | 2.89 | 2.50 | 2.24 |
| 6 | | 2456 | Pliocene | Mudstone | 7.47 | 14.22 | 4.98 | 2.50 | 3.12 |
| 7 | | 3352 | Pliocene | Mudstone | 5.10 | 13.31 | 3.40 | 2.50 | 2.36 |
| 8 | | 4245 | Pliocene | Mudstone | 5.72 | 16.15 | 3.81 | 2.50 | 2.73 |
| 9 | | 4608 | Pliocene | Siltstone | 4.63 | 11.77 | 3.09 | 2.70 | 2.29 |
| 10 | | 4875 | Pliocene | Siltstone | 2.62 | 17.20 | 4.10 | 2.70 | 2.25 |
| 11 | Hong-20 | 3315 | Oligocene | Mudstone | 2.60 | 7.40 | 0.56 | 2.50 | 1.14 |
| 12 | Hong-24 | 3243 | Oligocene | Sandstone | 5.00 | 1.61 | 0.74 | 2.70 | 1.47 |
| 13 | Hongshancan-1 | 910 | Cretaceous | Sandstone | 2.70 | 8.00 | 1.10 | 2.66 | 1.33 |
| 14 | Jian-2 | 1854 | Pliocene | Mudstone | 5.03 | 11.67 | 3.35 | 2.50 | 2.24 |
| 15 | | 1934 | Pliocene | Mudstone | 3.00 | 9.88 | 1.76 | 2.50 | 1.5 |
| 16 | | 2265 | Pliocene | Mudstone | 3.60 | 12.20 | 2.40 | 2.50 | 1.85 |
| 17 | Jiancan-1 | 3650 | Oligocene | Sandstone | 2.10 | 9.10 | 0.90 | 2.70 | 1.25 |
| 18 | Nan4 | 103 | Pliocene | Mudstone | 4.70 | 9.20 | 0.65 | 2.40 | 1.69 |
| 19 | Nan-7 | 1432 | Pliocene | Mudstone | 7.04 | 15.50 | 4.69 | 2.45 | 3.01 |
| 20 | Nan-8 | 2599 | Miocene | Mudstone | 4.77 | 14.63 | 3.18 | 2.50 | 2.35 |
| 21 | | 2971 | Miocene | Mudstone | 4.43 | 13.37 | 2.95 | 2.50 | 2.17 |
| 22 | Sezhong-6 | 393 | Quaternary | Mudstone | 5.20 | 12.45 | 3.47 | 2.42 | 2.26 |
| 23 | | 463 | Quaternary | Mudstone | 5.04 | 14.32 | 3.36 | 2.42 | 2.33 |
| 24 | | 518 | Quaternary | Mudstone | 4.58 | 14.20 | 3.05 | 2.42 | 2.19 |
| 25 | | 585 | Quaternary | Mudstone | 4.04 | 14.30 | 2.74 | 2.42 | 2.05 |
| 26 | | 643 | Quaternary | Mudstone | 4.86 | 19.00 | 3.24 | 2.42 | 2.57 |
| 27 | | 740 | Quaternary | Mudstone | 6.82 | 11.51 | 5.81 | 2.42 | 2.77 |
| 28 | | 833 | Quaternary | Mudstone | 3.89 | 20.77 | 2.59 | 2.42 | 2.4 |
| 29 | | 955 | Quaternary | Siltstone | 4.26 | 7.91 | 2.84 | 2.65 | 1.87 |
| 30 | | 1060 | Quaternary | Mudstone | 3.03 | 8.23 | 1.61 | 2.42 | 1.34 |
| 31 | Se-23 | 1206 | Quaternary | Mudstone | 4.38 | 15.37 | 2.92 | 2.42 | 2.21 |
| 32 | | 1296 | Quaternary | Mudstone | 7.36 | 10.44 | 4.91 | 2.42 | 2.76 |
| 33 | | 1460 | Pliocene | Mudstone | 3.65 | 12.03 | 2.43 | 2.42 | 1.79 |
| 34 | Shaxi-1 | 3009 | Pliocene | Sandstone | 2.72 | 4.90 | 0.85 | 2.70 | 1.12 |
| 35 | Shi-23 | 5500 | Oligocene | Sandstone | 5.82 | 9.07 | 3.88 | 2.70 | 2.49 |
| 36 | | 5510 | Paleocene | Sandstone | 4.20 | 9.60 | 0.70 | 2.70 | 1.81 |
| 37 | Shidi-22 | 672 | Jurassic | Siltstone | 4.00 | 1.56 | 0.90 | 2.70 | 1.22 |
| 38 | Xian-3 | 2906 | Oligocene | Sandstone | 3.90 | 1.90 | 1.66 | 2.70 | 1.29 |
| 39 | Xian-8 | 2768 | Miocene | Mudstone | 5.42 | 9.46 | 7.61 | 2.45 | 2.51 |
| 40 | | 3485 | Oligocene | Mudstone | 7.50 | 11.87 | 5.00 | 2.45 | 2.92 |
| 41 | | 3597 | Oligocene | Mudstone | 3.96 | 12.95 | 2.64 | 2.46 | 1.97 |
| 42 | | Outcrop | Jurassic | Sandstone | 4.10 | 11.20 | 1.90 | 2.70 | 2.01 |
| 43 | | Outcrop | Jurassic | Shale | 3.60 | 12.40 | 2.60 | 2.52 | 1.89 |
| 44 | | Outcrop | Carboniferous | Limestone | 2.10 | 1.40 | 0.30 | 2.70 | 0.665 |
| 45 | | Outcrop | Carboniferous | Limestone | 2.90 | 1.70 | 0.32 | 2.70 | 0.893 |
| 46 | | Outcrop | Proterozoic | Dolomite | 1.10 | 0.90 | 0.70 | 2.75 | 0.418 |
| 47 | | Outcrop | Ordovician | Limestone | 2.00 | 1.36 | 0.30 | 2.72 | 0.641 |
| 48 | | Outcrop | Triassic | Tuff | 4.60 | 11.10 | 1.00 | 2.73 | 2.07 |
| 49 | | Outcrop | Proterozoic | Marblite | 1.16 | 2.10 | 0.40 | 2.75 | 0.49 |
| 50 | | Outcrop | Proterozoic | Phylite | 4.60 | 8.70 | 0.72 | 2.75 | 1.89 |

U – uranium concentration, Th – thorium concentration, K – potassium concentration.

such as climate change, underground water and topography. We do not think other such perturbations are important in the heat flow calculated, since while these effects may result in a temperature change at some depth, they will not affect the regional thermal field. The second problem is to measure typical rock samples in order to get their thermal conductivities. The heat flow, calculated from systematic steady-state temperature data and thermal conductivities in the corresponding depth intervals, is called the 'measured' heat flow. Otherwise, the heat flow values are known as 'estimated' or 'calculated' heat flows. The measured heat flow data are the basis for studying the thermal regime of a region. However, estimated heat flow data can usually provide useful information as well, as long as the estimated heat flow is carefully obtained and reliable.

### 3.a. Geothermal gradients

The geothermal gradient data in this study are derived from systematic steady-state measurements, oil and gas testing, and temperature logging. The most important temperature data used to characterize the geothermal field of sedimentary basins are those from systematic steady-state temperature measurements and well tests. Theoretically, these temperature measurements are carried out with a 10 to 20 metre depth interval between

https://doi.org/10.1017/S0016756803008136 Published online by Cambridge University Press

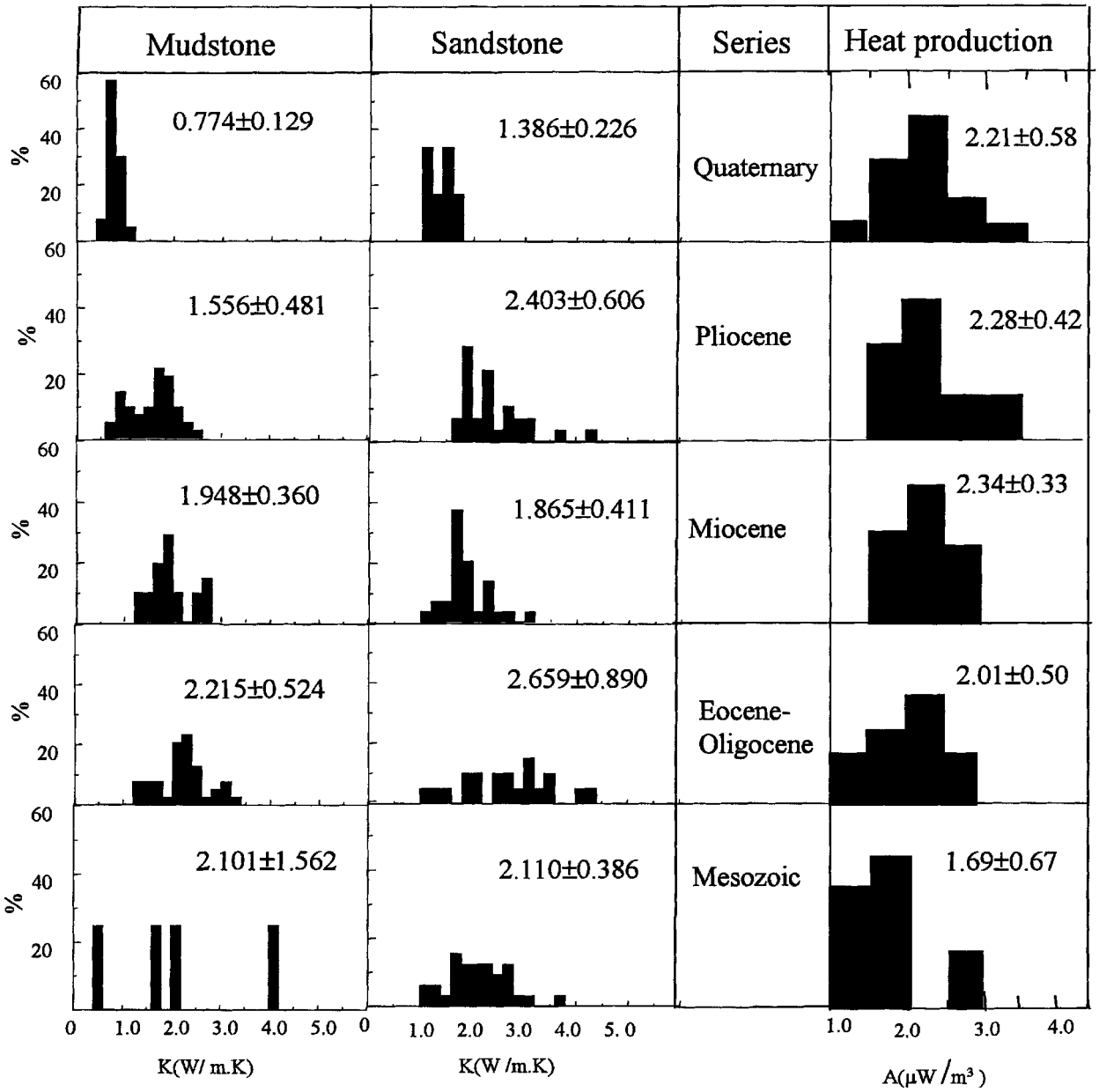


Figure 6. Histograms of thermal conductivities and radioactive heat production of rocks in Mesozoic and Cenozoic strata in the basin.

each test point, called 'systematic measurement'. However, the temperature would be greatly disturbed during drilling. Only after temperatures between the borehole fluid and surrounding rocks come to equilibrium, can the temperature field be called 'steady-state'. Usually, after a period equivalent to three to ten times the time interval required to drill the well, the surrounding rocks recover fully from the thermal perturbations caused by fluid movement. The tested temperature can then be regarded as the actual temperature. Twenty-two wells were selected to measure temperature systematically. These wells were all drilled one year or more prior to the temperature measurements, so that the temperature of the borehole fluid and the surrounding rocks could recover from thermal perturbations and return to the steady-state thermal profile. Systematic temperature measurements were carried out with a depth interval of 20 m, except in wells 3 and 5, and are called 'systematic steady-state measured temperatures' in this paper. Figure 7 illustrates temperature data from several wells (Shen *et al*. 1994*a*). Usually, convection within the stratum will result in some abnormal high and/or low temperature points in the profile. The temperature–depth profiles of the above wells show a good linear relationship between measured temperature and depth, showing the character of thermal conduction in the western basin.

The above steady-state temperature data are the basis for the thermal gradients. In addition, the temperature database for this study also includes abundant data from

https://doi.org/10.1017/S0016756803008136 Published online by Cambridge University Press

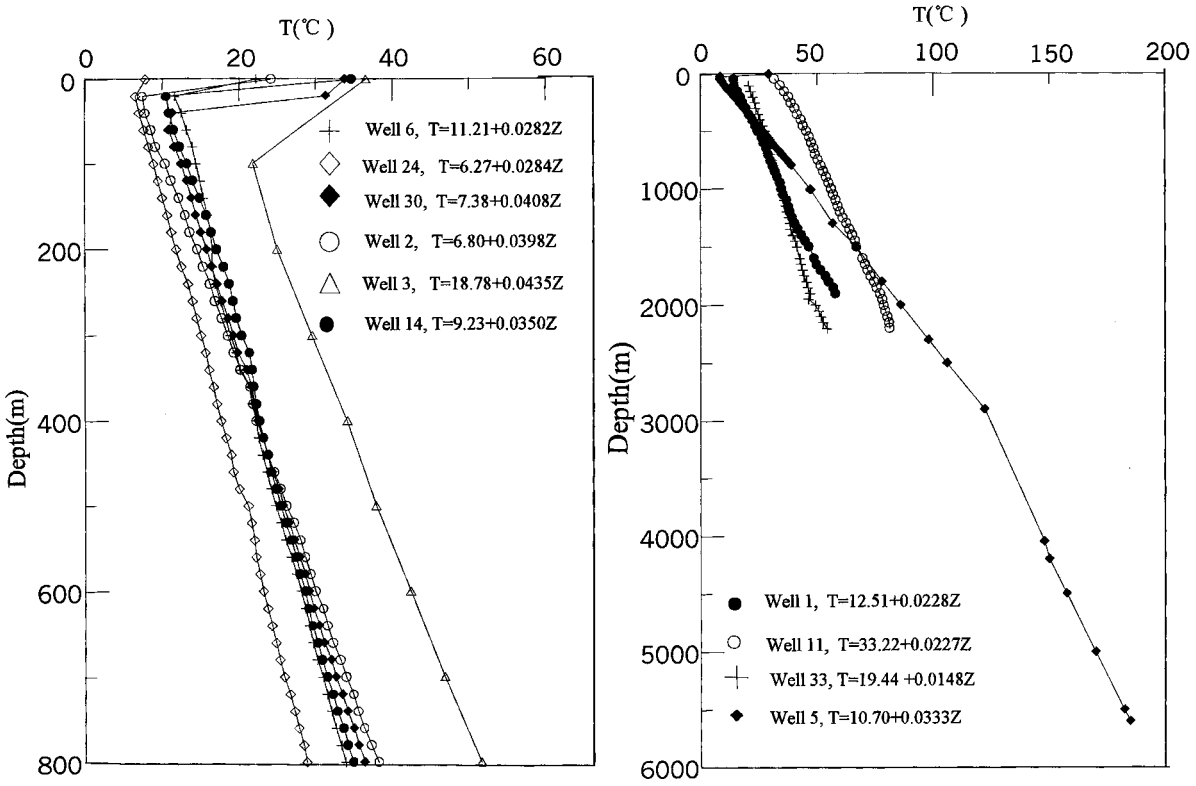


Figure 7. Temperature data from systematic steady-state measurement in ten wells (data from Shen *et al*. 1994*a*).

oil and gas testing and temperature logging provided by PetroChina Qinghai Petroleum Ltd, the sole operator for petroleum exploration and development in the Qaidam basin.

### 3.b. Thermal conductivity

The tested thermal conductivity values should be corrected to a water-saturated state when they are used to calculate heat flow. Li (G. H. Li, unpub. Masters thesis, Institute of Geology, Academia Sinica, 1992) tested 21 samples with water-saturated and original samples to obtain thermal conductivities. For original samples, the relationship between depth and thermal conductivity (K) is

$$K = 0.00058Z + 0.602 \quad (2)$$

and for water-saturated samples it is

$$K = 0.00036Z + 1.546 \quad (3)$$

When the sample depth is over 3000 m, however, the original samples and water-saturated samples show no difference in thermal conductivity. The conductivity values in each well were corrected to water-saturated values based on the water saturation correction formula (3), so that measured thermal conductivity reflected nearly *in situ* conditions. The conductivity values in Table 3 are all corrected for water saturation.

### 3.c. Heat flow calculation

Nineteen heat flow values were obtained from the systematic steady-state temperature measurement data and the water-saturated thermal conductivity values in the corresponding intervals of the same well (Table 3). These 19 heat flow values are 'measured heat flow' values. The heat flow values in wells 11, 12, 13, 19, 24, 28, 30 and 35 are comparable to the data from Shen *et al*. (1994*a*), but a discrepancy appears in some values, such as those from wells 1, 2, 6, 21 and 47. This difference may be attributed to the thermal conductivity data used to calculate heat flow in these wells. Shen *et al*. (1994*a*) gave the relationship between thermal conductivity and depth, then calculated heat flow by obtaining the thermal conductivity in the corresponding depth intervals from the depth-K relationship. However, there are many factors that would affect the thermal conductivity, including the rock type, its mineral composition and porosity. It is not appropriate to calculate the thermal conductivity from the formula obtained by regression. This explains the deviation between this study and the data of Shen *et al*. (1994*a*). The so-called measured heat flow should be calculated using the tested thermal conductivity and systematic steady-state temperature values.

Twenty-eight additional heat flow values, called estimated or calculated heat flows, were also obtained. Two situations may exist. (1) Only measured thermal conductivity data and/or oil test temperature data are

https://doi.org/10.1017/S0016756803008136 Published online by Cambridge University Press

Table 3. Heat flow values and heat generation data in the Qaidam basin

| Well no. | Well name | Depth intervals (m) | N | G (°C/km) | K (W/m · K) | q (mW/m$^2$) | | A ($\mu$W/m$^3$) | Heat flow | Data of Shen *et al.* (1994*a*) |
|---|---|---|---|---|---|---|---|---|---|---|
| 1 | Dacan-1* | 100–1400 | 1 | 27.7 | 1.469 | 40.7 | 38.5 ± 2.2 | | M | 24 |
| | | 1400–2800 | 1 | 23.7 | 1.532 | 36.3 | | | | |
| 2 | Dong-3* | 100–800 | 2 | 39.1 | 1.801 | 70.4 | 70.4 | | M | 122 |
| 3 | Feng-1* | 360–860 | 0 | 24.4 | 1.988 | 48.5 | 48.5 | | E | 37 |
| 4 | Feng-4 | 10–1671 | 1 | 27.0 | 2.053 | 55.4 | 54.6 ± 5.1 | | E | |
| | | 2525–2535 | 2 | 26.0 | 2.097 | 54.5 | | | | |
| | | 2535–3103 | 2 | 25.5 | 2.263 | 57.7 | | | | |
| | | 3103–4040 | 2 | 22.0 | 2.365 | 52.0 | | | | |
| 5 | Han-2* | 200–1955 | 2 | 33.0 | 1.954 | 64.5 | 63.9 ± 3.6 | 2.36 | M | 54 |
| | | 2456–3352 | 3 | 30.0 | 2.239 | 67.2 | | | | |
| | | 4245–4875 | 3 | 25.2 | 2.386 | 60.1 | | | | |
| 6 | Hong-27* | 360–800 | 0 | 29.3 | 1.741 | 51.0 | 51.0 | | E | 37 |
| 7 | Hong-102 | 0–744 | 2 | 32.0 | 1.769 | 56.6 | 56.2 ± 2.6 | 1.93 | E | |
| | | 744–1869 | 2 | 30.0 | 1.747 | 52.4 | | | | |
| | | 1869–1977 | 2 | 30.0 | 1.924 | 57.7 | | | | |
| | | 1977–2776 | 6 | 26.0 | 2.239 | 58.2 | | | | |
| 8 | Hongshancan-1 | 910–2100 | 4 | 22.0 | 1.920 | 42.2 | | 1.78 | E | |
| 9 | Jian-1 | 2625–2630 | 2 | 26.0 | 2.210 | 57.4 | 60.3 ± 2.9 | | E | |
| | | 3436–4182 | 3 | 22.0 | 2.873 | 63.2 | | | | |
| 10 | Jian-2 | 1844–2596 | 11 | 26.0 | 2.200 | 57.2 | 54.0 ± 3.3 | 1.93 | E | |
| | | 3000–4500 | 5 | 22.0 | 2.303 | 50.7 | | | | |
| 11 | Jiancan-1* | 712–1182 | 1 | 20.3 | 3.158 | 64.1 | 64.1 | | M | 62 |
| 12 | Leng-83* | 1570–2890 | 1 | 18.1 | 2.365 | 42.8 | 42.8 | | M | 43 |
| 13 | Leng-85* | 2835–3173 | 7 | 18.6 | 1.851 | 34.4 | 34.4 | 1.56 | M | 36 |
| 14 | Lucan-1* | 1785–2719 | 1 | 26.0 | 2.221 | 57.8 | 54.1 ± 5.8 | 2.31 | M | 61 |
| | | 2719–3324 | 1 | 25.0 | 2.289 | 57.2 | | | | |
| | | 3324–5092 | 5 | 24.0 | 1.973 | 47.4 | | | | |
| 15 | Manqian-1* | 150–450 | 1 | 15.7 | 1.994 | 31.3 | 31.3 | | M | 27 |
| 16 | Mazhong-20* | 460–620 | 1 | 17.1 | 2.101 | 35.9 | 35.9 | | M | 56 |
| 17 | Nan-4 | 102–1250 | 16 | 30.3 | 1.936 | 58.6 | 58.6 | 2.54 | E | |
| 18 | Nan-5 | 3020–3020 | 1 | 24.5 | 2.395 | 58.7 | 58.7 | | E | |
| 19 | Niucan-1* | 60–340 | 1 | 41.8 | 1.497 | 62.6 | 62.6 | | M | 63 |
| 20 | Saican-1 | 1022–1460 | 6 | 33.0 | 1.280 | 42.2 | 42.9 ± 0.7 | | E | |
| | | 1460–1650 | 2 | 33.0 | 1.321 | 43.6 | | | | |
| 21 | Sebeican-3* | 250–1400 | 1 | 33.8 | 1.155 | 39.0 | 39.0 | | M | 28 |
| 22 | Sezhong-6 | 382–1115 | 18 | 34.0 | 1.532 | 52.1 | 52.1 | 2.12 | E | |
| 23 | Sezhong-20 | 1032–1498 | 13 | 34.2 | 1.408 | 48.0 | 48.0 | | E | |
| 24 | Shi-22* | 20–800 | 1 | 28.7 | 1.892 | 54.3 | 54.3 | | M | 51 |
| 25 | Shi-23 | 3998–5683 | 13 | 23.0 | 2.356 | 54.2 | 54.2 | 2.15 | E | |
| 26 | Shidi-22 | 472–1200 | 6 | 22.0 | 2.000 | 44.0 | 44.0 | 1.24 | E | |
| 27 | Tainanz-3* | 30–1256 | 2 | 33.0 | 1.277 | 42.1 | 42.1 | | M | 35 |
| 28 | Tuozhong-2* | 318–875 | 7 | 25.8 | 1.764 | 45.5 | 45.5 | | M | 41 |
| 29 | Wanxi-1* | 0–293 | 2 | 28.8 | 2.086 | 60.1 | 60.7 ± 0.5 | | M | 56 |
| | | 293–1028 | 7 | 28.8 | 2.123 | 61.1 | | | | |
| | | 1018–3098 | 3 | 27.0 | 2.250 | 60.8 | | | | |
| 30 | Wu-7* | 60–800 | 0 | 33.9 | 1.540 | 52.2 | 52.2 | | M | 52 |
| 31 | Wu-8 | 2450–3305 | 3 | 22.0 | 2.524 | 55.5 | 55.5 | 2.20 | E | |
| 32 | Wu-12 | 1186–1521 | 8 | 28.0 | 2.221 | 62.2 | 62.2 | 3.13 | E | |
| 33 | Xian-2* | 10–170 | 1 | 28.0 | 1.989 | 55.7 | 55.2 ± 0.8 | | M | |
| | | 170–1500 | 3 | 28.0 | 2.000 | 56.0 | | | | |
| | | 1500–2400 | 2 | 26.4 | 2.061 | 54.4 | | | | |
| | | 2400–2770 | 1 | 24.4 | 2.246 | 54.8 | | | | |
| 34 | Xian-3 | 1793–2308 | 3 | 28.0 | 2.093 | 58.6 | 53.5 ± 5.1 | 2.00 | E | 62 |
| | | 2308–2908 | 2 | 27.0 | 1.791 | 48.4 | | | | |
| 35 | Xianzhong-8* | 25–870 | 1 | 17.3 | 1.902 | 32.9 | 32.9 | | M | 29 |
| 36 | Yacan-3 | 1883–2080 | 2 | 30.0 | 2.039 | 61.2 | 57.1 ± 4.7 | 2.25 | E | |
| | | 2180–4278 | 12 | 26.0 | 2.230 | 58.0 | | | | |
| | | 4631–4918 | 2 | 25.1 | 2.072 | 52.0 | | | | |
| 37 | Yanxin-1 | 135–348 | 7 | 30.8 | 1.692 | 52.1 | 52.1 | | E | |
| 38 | Yue-12 | 1200–1815 | 4 | 30.0 | 1.960 | 58.8 | 58.8 | | E | |
| 39 | Yue-58 | 1780–1945 | 2 | 32.0 | 1.880 | 60.2 | 61.4 ± 1.2 | | E | |
| | | 1945–2130 | 2 | 32.0 | 1.957 | 62.6 | | | | |
| 40 | Yue-119 | 3253–3425 | 3 | 25.1 | 2.333 | 58.6 | 58.6 | | E | |
| 41 | Yue-127 | 3669–3935 | 3 | 25.5 | 2.241 | 57.1 | 57.1 | 2.08 | E | |
| 42 | Yuedong-30* | 3516–3701 | 4 | 32.1 | 2.120 | 68.0 | 68.0 | 2.70 | M | 63 |
| 43 | Yuehui-1 | 3218–3256 | 3 | 26.0 | 2.215 | 57.6 | 57.6 | 2.39 | E | |
| 44 | Yuezhong-65 | 1360–1455 | 4 | 30.0 | 2.273 | 68.2 | 65.5 ± 2.7 | 2.27 | E | |
| | | 1455–2001 | 24 | 30.0 | 2.094 | 62.8 | | | | |

https://doi.org/10.1017/S0016756803008136 Published online by Cambridge University Press

Table 3. (*Cont.*)

| Well no. | Well name | Depth intervals (m) | N | G (°C/km) | K (W/m · K) | q (mW/m$^2$) | | A ($\mu$W/m$^3$) | Heat flow | Data of Shen *et al.* (1994*a*) |
|---|---|---|---|---|---|---|---|---|---|---|
| 45 | You-6 | 1936–2877 | 2 | 29.0 | 1.789 | 51.9 | 53.7 ± 1.8 | | E | |
| | | 2877–4311 | 2 | 23.5 | 2.363 | 55.5 | | | | |
| 46 | You-14 | 1977–2896 | 2 | 28.2 | 2.155 | 60.8 | 60.7 ± 0.0 | 2.02 | E | |
| | | 2896–3002 | 2 | 28.2 | 2.153 | 60.7 | | | | |
| 47 | Youzhong-3* | 1720–2020 | 0 | 28.2 | 1.943 | 54.8 | 54.8 | | E | 41 |

*Wells with steady-state temperature measurements. M – measured heat flow value; E – estimated heat flow; N – number of thermal conductivity samples tested; K – thermal conductivity with water saturation correction; G – thermal gradient; q – heat flow value; A – heat generation.

available, whereas systematic steady-state temperature measurement data are not available. In this case, thermal gradients are calculated based on the oil and gas testing and logging temperature data. (2) Steady-state temperature measurement data are available, whereas tested thermal conductivity values are not obtained, as in wells 3, 6 and 47. In this case, the heat flow values are calculated by applying the thermal conductivity data from the same stratigraphic interval in nearby wells. Figure 6 shows the histogram of thermal conductivity for the two main kinds of rocks in the Mesozoic and Cenozoic strata. To calculate the heat flow of a well with only thermal gradient data, we can use the thermal conductivity of the corresponding stratum in the wells nearby. Since wells 6, 24 and 47 have no measured thermal conductivity data, the heat flow values in these wells have also been calculated.

The heat flow in the Qaidam basin ranges from 31.3 to 70.4 mW/m$^2$ (Table 3). The statistical average for the 47 heat flow values in the basin is 52.6 ± 9.6 mW/m$^2$. This is lower than that of the basins in eastern China, where the average heat flow value is more than 60 mW/m$^2$ (Wang, 1996), but higher than the average value of 44.05 mW/m$^2$ found in the Tarim Basin (Wang *et al*. 1995).

A heat flow contour map of the basin was constructed based on the 19 measured heat flow values (Fig. 8). When the estimated or calculated heat flow values are also included on the map, however, the heat flow distribution characteristics do not change, indicating that the estimated or calculated heat flow values are reliable. The following thermal structure analysis is based on the measured and calculated heat flow values. Well 2 has an abnormally high heat flow, but this high value does not disturb the heat-flow distribution pattern of the basin. The heat flow is higher in the western and central parts of the basin (> 60 mW/m$^2$), and lower in the eastern and northern parts of the basin, lower than 40 mW/m$^2$ at the basin margins.

## 4. Thermal structure analysis

It is well known that heat is generated by two sources. One is the radioactive decay of uranium (U), thorium (Th) and potassium (K) at relatively shallow depths; the other is from mantle heat flow. Birch, Roy & Decker (1968) first discovered that the total terrestrial heat flow observed at the Earth's surface emanates from two sources: the radiogenic heat produced by the decay of radioactive elements (U, Th, $^{40}$K) in the uppermost part of the crust, and the heat flow from the lower crust and upper mantle. They used a linear formula to describe these two sources of heat flow, which made separation of the two components (crust and mantle heat flow) possible. Roy *et al*. (1968) defined a 'heat flow province' as a region with the same heat flow from the mantle. Blackwell (1971) first used the term 'thermal structure of the continental crust' to describe an area with a certain heat flow value and thus a particular ratio of mantle to surface heat flow and/or crust to mantle heat flow. The thermal structure may be determined from the measured heat flow in a region based on the data from surface heat flow and heat production. We analysed the thermal structure of the Qaidam basin based on the surface heat flow and heat production data by applying the linear formula of Birch, Roy & Decker (1968):

$$q = q_m + DA = q_m + q_c \quad (4)$$

where q is the heat flow at the surface, D is the depth of the radioactive element concentration layer in the upper crust, $q_m$ is the mantle heat flow, $q_c$ is the heat flow from radioactive heat production in relatively shallow depths of the crust, and A is the heat production of rocks in which the heat flow measurement was expressed in $\mu$W/m$^3$.

Heat flow values at the surface and heat production values of rocks may vary in different areas, if the values of $q_m$ and D are the same in a given region; this indicates that the heat flow coming from the mantle is uniform across the region, and the thicknesses of radioactive element concentration layers are the same, indicating that the basin or region has had the same geological and geochemical history. However, different geological units may have different $q_m$ and D values (Jessop & Judge, 1971; Blackwell, 1971; Jaeger, 1970).

For this study, heat flow values and measured heat production data are both available for 19 wells (Table 3). These heat flow and radioactive heat production values

https://doi.org/10.1017/S0016756803008136 Published online by Cambridge University Press

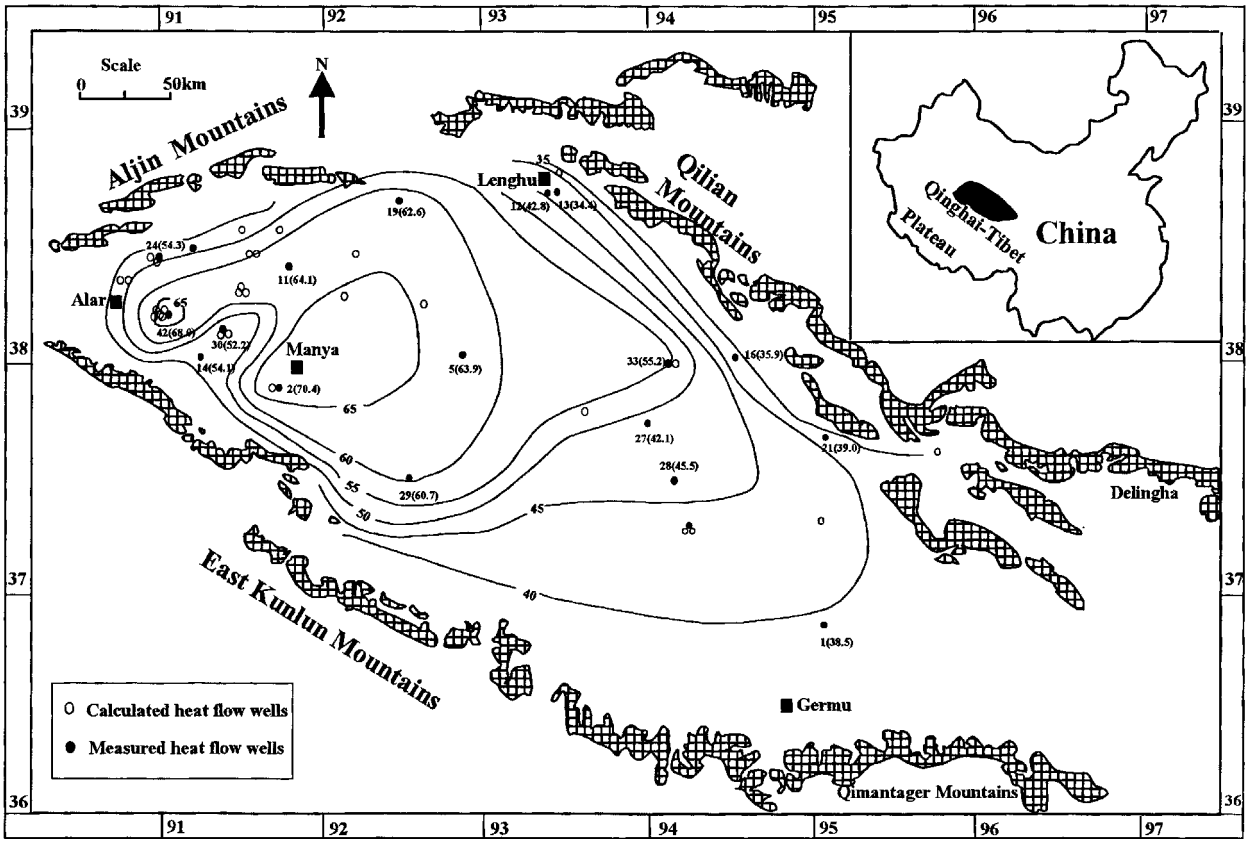


Figure 8. Contour map of heat flow in the Qaidam basin based on the measured heat flow values. The solid circles indicate the wells with measured heat flow values (mW/m$^2$) with well numbers and heat flow values in parentheses.

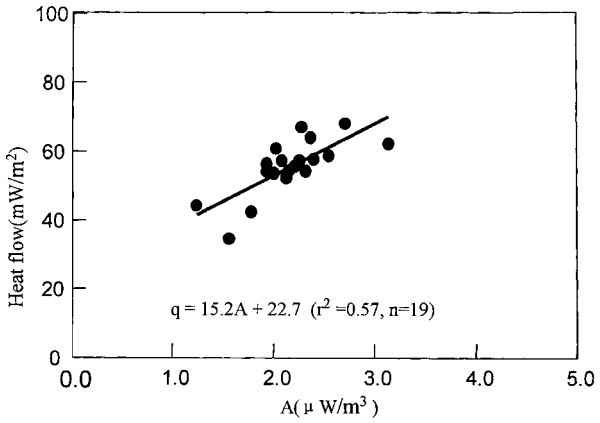


Figure 9. Relationship between heat flow and heat production in 19 wells.

were analysed according to the above linear formula. A linear regression formula was obtained (Fig. 9):

$$q = 22.7 + 15.2A \quad (r^2 = 0.57,\ n = 19) \qquad (5)$$

Based on the work of Birch, Roy & Decker (1968), heat flow from the mantle in the Qaidam basin is 22.7 mW/m$^2$, constituting only 43.2 % of the total surface heat flow (52.6 mW/m$^2$). However, the radioactive heat flow may contribute up to 29.9 mW/m$^2$, more than from the mantle and constituting 56.8 % of the total surface heat flow. The mantle here possesses the characteristics of a so-called 'cold mantle', a term defined by Wang (1996), and the crust is a relative 'hot crust'. The D value is 15.2 km in this region, which implies a relatively large thickness for the concentration layer of radioactive elements. This result indicates that the Qaidam basin is characterized by a 'hot crust' but 'cold mantle', and here, the Qaidam basin is identified as a heat flow province.

## 5. Discussion

Nineteen measured heat flow values were obtained for this study, while Shen *et al*. (1994*a*) obtained 22 heat flow values in the wells from steady-state temperature measurement data. These data give the relationship between thermal conductivity and depth, allowing heat flow to be calculated from the thermal conductivity in the corresponding depth intervals with depth-K relationship regression formulas. These heat flow values are not 'measured heat flow values', strictly speaking. For this study, 28 estimated heat flow values were calculated by applying the thermal conductivity data from the same stratigraphic interval in nearby wells and the measured temperature data (Fig. 6). The results

https://doi.org/10.1017/S0016756803008136 Published online by Cambridge University Press

obtained by this method may be more reliable those of Shen *et al*. (1994*a*).

Because the Himalayan region was highly active in Quaternary times, the crust may not be at thermal equilibrium today. This results in higher heat-flow in the crust to some extent. Tectonic movements induce thermal disequilibrium in the crust and sometimes in the mantle. The 'hot crust'/'cold mantle' structure of the Qaidam basin also reflects the tectonic movement and the thermal disequilibrium of the crust.

The linear q-A relationship is a feature of the thermal state of a continuously evolved lithosphere. Since the q-A linear relationship was first discovered in a plutonic batholith in New England, USA, this relationship has been found to be valid for other metamorphic rocks and terrains in different parts of the world. However, when it is used to study sedimentary basins, there are still some limitations which result in a poorer fit to a linear relationship and lower correlation coefficient, for example, $r^2 = 0.57$ in this study. Lee *et al*. (1987) also obtained a low $r^2$ value for the q-A linear relationship when they studied a heat flow province on the mainland of Britain. In our study, we use all our calculated heat flow values to analyse the q-A relationship, which may result in the lower $r^2$ value. In fact, the distribution of radiogenic heat production in the upper to middle crust is complex, and the provenance of sediments in different stratigraphic intervals may be different. As a result, there may be no relationship between the upper and lower sedimentary successions, which renders the exponential model of radiogenic heat production distribution invalid or inaccurate (Zhao & Wang, 1995). Tested heat production is apparently distributed uniformly in the Cenozoic strata, also indicating that radioactive elements are concentrated in the upper crust of the Qaidam region.

Heat production in the sedimentary section is thought to be significant, and we agree with Keen & Lewis (1982) that heat production should be included in thermal modelling of the basin. The concentration layer, D, of radioactive elements has a relatively large thickness of over 15 km in the Qaidam region. This also indicates that the heat production should be included in the thermal model of the basin. The heat flow due to heat production in the crust can contribute 29.9 $mW/m^2$. On the one hand, this is important when calculating the temperature in the deep crust based on steady-state conduction models. On the other hand, the role of heat production should be included when reconstructing the thermal history of the basin.

## 6. Conclusions

Ninety-eight thermal conductivity and 50 heat production values were tested for this study. These measurements and the data of other workers provide information about thermal conductivity and heat production of the rocks in the upper crust of the Qaidam basin and thereby the Qinghai–Tibet Plateau. Nineteen measured heat flows were obtained based on detailed thermal conductivity data and systematic steady-state temperature data; this paper also contributes 28 calculated heat flow values for the basin. These values were found to be between 31.3 to 70.4 $mW/m^2$ with an average value of $52.6 \pm 9.6$ $mW/m^2$, which is relatively lower than that of other basins in eastern China (Wang, 1996). Heat flow values higher than 60 $mW/m^2$ are distributed through the western and central parts of the basin; lower heat flows are found in the eastern part and the northern marginal area of the basin, with values less 40 $mW/m^2$.

The Qaidam basin heat flow province is identified for the first time based on the q-A relationship derived from thermal structure analysis of the heat flow and heat production data using the approach of Birch, Roy & Decker (1968). The thermal structure in this area shows the characteristics of a 'hot crust' but 'cold mantle'. Wang & Huang (1991) identified the first heat flow province in China based on the q-A relation. In this study, the terms 'heat flow province' and 'thermal structure of the lithosphere' are considered to be essentially identical because the key criteria defining these two terms are regarded as being the same as the mantle heat flow. A 'heat flow province' may be regarded as a region with a certain mantle heat flow and a similar lithospheric thermal structure.

The heat flow province is of great geophysical significance. The thermal structure of a region gives an indication of the relative levels of crust and mantle 'activity'. The 'cold mantle'/'hot crust' thermal structure of the lithosphere in the Qaidam region shows that the crust has been highly active, particularly in the later stages of the geological evolution of the basin. This thermal structure also corresponds to the Himalayan tectonic movement from latest Eocene to Quaternary times in the Qinghai–Tiebet Plateau region. As the Qaidam basin is located in the northeastern part of Qinghai–Tibet Plateau, the thermal structure and evolution of the basin may say something about the structure, evolution and tectonic charateristics of the entire plateau.

**Acknowledgements.** Grateful acknowledgements are made to PetroChina Qinghai Petroleum Ltd and individuals who contributed cores and information for this work. The China National Natural Science Foundation (grant no. 40125008), National Major Fundamental Research and Development Project (G1999043302) and CNPC (9702080401) provided financial support. The Laboratory for Geothermics, Institute of Geology, Academia Sinica, tested thermal conductivity and heat production of the samples. Professors Zhang Yiwei, Xiong Jihui, Jin Zhijun, Zhu Xiaomin and Tang Lianjie gave helpful comments and suggestions during the research work. My heartfelt gratitude also goes to Drs Kevin Burke, Shaopeng Huang, Guoping Bai and two anonymous referees for their scientific and linguistic revisions of the manuscript.

## References


BECK, A. E. & BALLING, N. 1988. Determination of virgin rock temperature. In *Handbook of terrestrial heat flow density determination* (eds R. Haenel, L. Rybach and L. Stegena), pp. 59–86. Dordrecht: Kluwer Academic Publishers.

BIRCH, F., ROY, R. F. & DECKER, E. R. 1968. Heat flow and thermal history in New York and New England. In *Studies of Appalachian Geology: Northern and Maritime* (eds E. Zen, W. S. While, J. B. Hadley and J. B. Thompson), pp. 437–51. New York: Interscience.

BLACKWELL, D. D. 1971. The thermal structure of the continental crust. In *Structure and physical properties of the Earth's Crust* (ed. J. G. Heacock), pp. 169–84. Washington, D.C.: American Geophysical Union.

GAO, R. Q. & ZHAO, Z. Z. 2001. *The frontier petroleum exploration in China. Vol. 6, Petroleum Geology of Qinghai–Tibet Plateau.* Beijing: Petroleum Industry Press.

HUANG, X. Z. 1993. *Hydrocarbon generation and exploration in Qaidam basin.* Lanzhou: Gansu Science & Technology Press, 266 pp. (in Chinese).

HUANG, H. C., HUANG, Q. H. & MA, Y. S. 1996. *Geology and petroleum prediction in Qaidam basin.* Beijing: Geological Press, 205 pp. (in Chinese).

JAEGER, J. C. 1970. Heat flow and radioactivity in Australia. *Earth and Planetary Science Letters* **8**, 285–92.

JESSOP, A. M. & JUDGE, A. S. 1971. Five measurements of heat flow in Southern Canada. *Canadian Journal of Earth Sciences* **8**, 711–16.

KEEN, C. E. & LEWIS, T. 1982. Measured radiogenic heat production in sediments from continental margin of eastern North America: implications for petroleum generation. *Bulletin of the American Association of Petroleum Geologists* **66**, 1402–7.

LEE, M. K., BROWN, G. C., WEBB, P. C., WHEILDON, J. & ROLLIN, K. E. 1987. Heat flow, heat production and thermal-tectonic setting in mainland UK. *Journal of the Geological Society, London* **144**, 35–42.

QIU, N. S. 2002. Thermal-tectonic evolution of the Qaidam basin, Northeast Qinghai-Tibet Plateau – evidence from Ro and Apatite fission track data. *Petroleum Geosciences* **8**(3), 279–85.

REN, Z. L. 1993. Thermal evolution history in Qaidam basin: Evidence from fluid inclusions and Ro data. In *Developments in oil and gas basin geology* (eds C. Y. Zhao, C. Y. Liu, Y. Yao *et al*.), pp. 235–47. Xi-an: Northwest University Press (in Chinese).

ROBERTSON, E. C. 1988. Thermal properties of rocks. *U.S. Geological Survey Open-File Report*, pp. 88–441.

ROY, R. F., DECKER, E. R., BLACKWELL, D. D. & BIRCH, F. 1968. Heat generation of plutonic rocks and continental heat flow province. *Earth and Planetary Science Letters* **5**, 1–12.

SHEN, X. J., LI, G. H., WANG, J. A., DEN, X., ZHANG, W. R. & YANG, S. Z. 1994*a*. Terrestrial heat flow and statistical heat flow calculation in Qaidam basin, Qinghai Province (in Chinese). *Acta Geophysica Sinica* **37**, 56–65.

SHEN, X. J., WANG, J. A., ZHANG, J. M., DEN, X., YANG, S. Z. & ZHANG, W. R. 1994*b*. Burial, thermal and maturation histories simulation and oil-gas prospect prediction in Qaidam basin, Qinghai Province. *Chinese Science Bulletin* **39**, 836–41.

SHEN, X. J. & WANG, J. A. 1995. Mechanism of petroleum maturation history controlled by burial history – a case history of Qaidam basin. *Chinese Science Bulletin (B)* **25**, 441–8.

TOULOUKIAN, Y. S. & DEWITT, D. P. 1972. Thermal radioactive properties-nonmetallic solids. In *Thermophysical properties of matter*, 8 (eds Y. S. Touloukian and C. Y. Ho), pp. 28–56. New York: Plenum Press.

WANG, J. Y. 1996. *Geothermics in China.* Beijing: Seismological Press.

WANG, J. Y. & HUANG, S. P. 1991. The thickness of the thermal lithosphere in the Panxi Paleorift Zone, southwestern China. In *Terrestrial heat flow and the lithosphere structure* (eds V. Cermark and L. Rybach), pp. 308–16. Berlin: Springer-Verlag.

WANG, J., HUANG, G. S., HUANG, S. Y. & WANG, J. Y. 1990. *Basic characteristics of the Earth's temperature distribution in China.* Beijing: Seismological Press, 299 pp.

WANG, J., WANG, J. A., SHEN, J. Y. & QIU, N. S. 1995. Heat flow in Tarim basin. *Earth Science – Journal of China University of Geosciences* **20**, 399–404.

ZHAO, P. & WANG, J. Y. 1995. Review on the linear heat flow production relation. *Progress in Geophysics* **10**, 16–31.


https://doi.org/10.1017/S0016756803008136 Published online by Cambridge University Press